Limits to the muon flux from neutralino annihilations in the Sun with the AMANDA detector

M. Ackermann [a], J. Ahrens [b], X. Bai [c], M. Bartelt [d], S.W. Barwick [e], R.C. Bay [f], T. Becka [b], K.-H. Becker [g], J.-K. Becker [d], P. Berghaus [h], E. Bernardini [a], D. Bertrand [h], D.J. Boersma [a], S. Böser [a], O. Botner [i], A. Bouchta [i], O. Bouhali [h], C. Burgess [j], T. Burgess [j], T. Castermans [k], D. Chirkin [f], B. Collin [l], J. Conrad [i], J. Cooley [m], D.F. Cowen [l], M. D'Agostino [f], A. Davour [i], C. De Clercq [n], C.P. de los Heros [i,*], T. DeYoung [o], P. Desiati [m], P. Ekström [j], T. Feser [b], T.K. Gaisser [c], R. Ganugapati [m], H. Geenen [g], L. Gerhardt [e], A. Goldschmidt [p], A. Gross [d], A. Hallgren [i], F. Halzen [m], K. Hanson [l], D.H. Hardtke [f], T. Harenberg [g], T. Hauschildt [c], M. Hellwig [b], K. Helbing [p], P. Herquet [k], G.C. Hill [m], J. Hodges [m], D. Hubert [n], B. Hughey [m], P.O. Hulth [j], K. Hultqvist [j], S. Hundertmark [j], J. Jacobsen [p], K.H Kampert [g], A. Karle [m], M. Kestel [l], G. Kohnen [k], L. Köpke [b], M. Kowalski [a], K. Kuehn [e], R. Lang [a], H. Leich [a], M. Leuthold [a], I. Liubarsky [q], J. Lundberg [i], J. Madsen [m], P. Marciniewski [i], H.S. Matis [p], C.P. McParland [p], T. Messarius [d], Y. Minaeva [j], P. Miočinović [f], R. Morse [m], K. Münich [d], R. Nahnhauer [a], J.W. Nam [e], T. Neunhöffer [b], P. Niessen [c], D.R. Nygren [p], H. Ögelman [m], Ph. Olbrechts [n], A. Pohl [r], R. Porrata [f], P.B. Price [f], G.T. Przybylski [p], K. Rawlins [m], E. Resconi [a], W. Rhode [d], M. Ribordy [k], S. Richter [m], S. Robbins [g], J. Rodríguez Martino [j], H.-G. Sander [b], S. Schlenstedt [a], D. Schneider [m], R. Schwarz [m], A. Silvestri [e], M. Solarz [f], G.M. Spiczak [s], C. Spiering [a], M. Stamatikos [m], D. Steele [m], P. Steffen [a], R.G. Stokstad [p], K.-H. Sulanke [a], I. Taboada [f], O. Tarasova [a], L. Thollander [j], S. Tilav [c], W. Wagner [d], C. Walck [j], M. Walter [a], Y.-R. Wang [m], C.H. Wiebusch [g], R. Wischnewski [a], H. Wissing [a], K. Woschnagg [f]

---

* Corresponding author.
  E-mail address: cph@tsl.uu.se (C.P. de los Heros).

^a *DESY, Platanenallee 6, D-15738 Zeuthen, Germany*
^b *Institute of Physics, University of Mainz, D-55099 Mainz, Germany*
^c *Bartol Research Institute, University of Delaware, Newark, DE 19716, USA*
^d *Institute of Physics, University of Dortmund, D-44221 Dortmund, Germany*
^e *Department of Physics and Astronomy, University of California, Irvine, CA 92697, USA*
^f *Department of Physics, University of California, Berkeley, CA 94720, USA*
^g *Department of Physics, University of Wuppertal, D-42119 Wuppertal, Germany*
^h *Université Libre de Bruxelles, Science Faculty CP230, B-1050 Brussels, Belgium*
ⁱ *Division of High Energy Physics, Uppsala University, S-75121 Uppsala, Sweden*
^j *Department of Physics, Stockholm University, S-10691 Stockholm, Sweden*
^k *Faculty of Sciences, University of Mons-Hainaut, B-7000 Mons, Belgium*
^l *Department of Physics and Astronomy, Pennsylvania State University, University Park, PA 16802, USA*
^m *Department of Physics, University of Wisconsin—Madison, Madison, WI 53706, USA*
ⁿ *Vrije Universiteit Brussel, Dienst ELEM, B-1050 Brussels, Belgium*
^o *Department of Physics, University of Maryland, College Park, MD 20742, USA*
^p *Lawrence Berkeley National Laboratory, Berkeley, CA 94720, USA*
^q *Blackett Laboratory, Imperial College, London SW7 2BW, UK*
^r *Department of Chemistry and Biomedical Sciences, University of Kalmar, SE-39182 Kalmar, Sweden*
^s *Department of Physics, University of Wisconsin—River Falls, River Falls, WI 54011, USA*

Abstract

A search for an excess of muon–neutrinos from neutralino annihilations in the Sun has been performed with the AMANDA-II neutrino detector using data collected in 143.7 days of live-time in 2001. No excess over the expected atmospheric neutrino background has been observed. An upper limit at 90% confidence level has been obtained on the annihilation rate of captured neutralinos in the Sun, as well as the corresponding muon flux limit at the Earth, both as functions of the neutralino mass in the range 100–5000 GeV.
© 2005 Elsevier B.V. All rights reserved.

Keywords: Dark matter; Neutrino telescopes; AMANDA; Neutralino

1. Introduction

The minimal supersymmetric extension to the standard model of particle physics (MSSM) [1] provides a promising dark matter candidate in the lightest neutralino, $\tilde{\chi}_1^0$, a linear combination of the supersymmetric partners of the electroweak neutral gauge and Higgs bosons. Assuming R-parity conservation, the neutralino is stable. From accelerator searches and relic density constraints from WMAP data, a lower limit on the mass of the MSSM neutralino can be derived [2]. Typical lower limits for $m_{\tilde{\chi}_1^0}$ from such studies are about 20 GeV, depending on the values chosen for $\tan \beta$. In models where the pseudo-scalar Higgs boson A

is assumed to be light, $m_A < 200$ GeV, the neutralino mass can be as low as 6 GeV. Theoretical arguments based on the requirement of unitarity set an upper limit on $m_{\tilde{\chi}_1^0}$ of 340 TeV [3]. Within these limits, the allowed parameter space of minimal supersymmetry can be exploited to build realistic models which provide relic neutralino densities of cosmological interest to address the dark matter problem.

Relic neutralinos in the galactic halo can become gravitationally bound in orbits in the solar system by losing energy through elastic scattering with matter. They may finally be trapped and accumulate inside celestial bodies like the Sun [4–6], annihilate, and produce a neutrino flux from the decays of the annihilation products [7].

We have previously published a search for neutralino dark matter accumulated in the Earth using the 10-string detector AMANDA-B10 and data from 1997 [8]. In this article we present the first search for neutralino dark matter accumulated in the Sun with the extended AMANDA-II detector. Due to the position of the Sun at the South Pole, reaching no more than 23.5° below the horizon, the separation of a potential neutralino-induced neutrino flux from the Sun from the atmospheric muon flux is a challenge that we could only address because of the increased sensitivity of the AMANDA-II detector to horizontal tracks.

2. The AMANDA-II detector

AMANDA-II consists of an array of 677 optical modules deployed on 19 vertical strings at depths between 1500 m and 2000 m in the South Pole ice cap. The strings are arranged in three approximately concentric circles of 60 m, 120 m and 200 m diameter, respectively. An optical module consists of a photomultiplier tube housed in a glass pressure vessel. Muons from charged-current neutrino interactions near the array are detected by the Cherenkov light they produce when traversing the ice. During 2001 the detector was triggered when at least 24 modules were hit within a time window of 2.5 μs. The trigger rate was 70 Hz. The relative timing of the photons reaching the optical modules allows the reconstruction of the muon track. A more detailed description of the reconstruction techniques used in AMANDA is given in Ref. [9].

3. Signal and background simulations

The simulation of the neutralino-induced neutrino signal was performed using the DARKSUSY program [10] for a sample of neutralino masses (100, 250, 500, 1000, 3000 and 5000 GeV). Neutralinos can annihilate pair-wise to, e.g., $\ell^+\ell^-$, $q\bar{q}$, W^+W^-, Z^0Z^0, $H^0_{1,2}H^0_3$, $Z^0H^0_{1,2}$ and $W^\pm H^\mp$, and neutrinos are produced in the decays of the annihilation products. Neutrinos produced in quark jets (from e.g. $b\bar{b}$) or from Higgs bosons typically have lower energy than those produced

from decays of τ leptons or gauge bosons. Two annihilation channels were considered in this paper for each mass tested, $\widetilde{\chi}^0_1\widetilde{\chi}^0_1 \rightarrow b\bar{b}$ and $\widetilde{\chi}^0_1\widetilde{\chi}^0_1 \rightarrow W^+W^-$, which are referred to as *soft* and *hard*, respectively, in the rest of the paper. This choice covers the range of neutrino energies which would be detectable with AMANDA for typical MSSM models. The simulated angular range was restricted to zenith angles between 90° (horizontal) and 113°, with the generated number of events as a function of angle weighted by the time the Sun spends at each declination. The neutrino–nucleon interactions in the ice around the detector producing the detectable muon flux were simulated with PYTHIA [11] using the CTEQ3 [12] parameterization of the nucleon structure functions.

The background for this search arises from upgoing atmospheric neutrinos and mis-reconstructed downward-going atmospheric muons. We have simulated the atmospheric neutrino flux according to [13]. The simulation includes neutrino propagation through the Earth, taking into account the Earth density profile, neutrino absorption and neutral current scattering. A sample of 1.9×10^4 atmospheric neutrinos with energies between 10 GeV and 10 PeV and zenith angles between 70° and 180° (vertically up-going) has been simulated. The simulation of atmospheric muons was based on the CORSIKA air shower generator [14] using the South Pole atmosphere parameters and protons as primaries. We have simulated 1.6×10^8 interactions, distributed isotropically with zenith angles between 0° and 85°, and with proton energies, E_p, between 600 GeV and 10^{11} GeV, assuming a differential energy distribution $\propto E_p^{-2.7}$ [15]. The sample corresponds to about 32.5 days of equivalent detector live-time.

Muons were propagated from the production point to the detector taking into account energy losses by bremsstrahlung, pair production, photonuclear interactions and δ-ray production as implemented in the code MMC [16].

4. Data analysis

The dataset used comprises 8.7×10^8 events collected in 143.7 days of effective live-time between

the end of March and the end of September 2001. The data and Monte Carlo events have been reconstructed with a fast first-guess track finding algorithm which is used as a seed for an iterative maximum-likelihood reconstruction. The reconstructed events were processed through a series of filters in order to reduce the atmospheric muon background and retain as much of a potential signal as possible. The variables used in the analysis are the same for the different neutralino masses, but the cuts have been optimized independently for each mass in order to exploit the differences in the resulting muon energy spectra. The event selection was optimized in a 'blind' way, by explicitly excluding the time tag of the events (and thus the direction of the Sun) in the development of the selection criteria (see [17] for details of this analysis).

Firstly, events were selected according to the quality of the track reconstruction and their zenith angle. The quality criteria were based on 'direct hits', i.e. hits with time residuals, t_{res}, in the interval [−15 ns, 25 ns] relative to the expected arrival time of an unscattered photon from the fitted track. Cuts were made on the number of direct hits, the maximum distance along the track direction between two such hits and the number of strings with direct hits. This selection (cut levels 1–3 in Fig. 1) resulted in a rejection of 99.97% of the data (mostly down-going muons), while the simulated background from atmospheric neutrinos was reduced to 30%. The simulated signal was reduced between 46% and 54% (depending on the neutralino mass).

The next step consisted on a cut on a neural network (NN) output. For each neutralino mass, a NN was optimized for the simulated signal and a background sample consisting of simulated atmospheric muons. No information about the characteristics of atmospheric neutrinos was included in the training of the network. Eight variables were used as an input to the NN to characterize the events: the number of hit channels, the difference in reconstructed angle between the fast first-guess fit and the maximum likelihood fit, the number of 'late' ($t_{res} > 150$ ns) hits, the track length of the first-guess fit, the length spanned by all the hits projected onto the direction of the final recon-
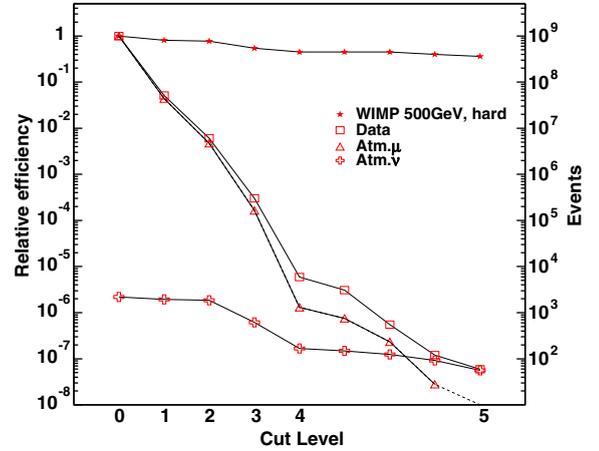

Fig. 1. Relative cut efficiencies for one of the neutralino masses and annihilation channels considered in this paper, 500 GeV hard. The efficiency is set to 1 at trigger level, except for the atmospheric neutrino curve, that has been scaled relative to the number of events expected in the live-time of the analysis. The axis scale on the right gives the absolute normalization for the data and the atmospheric neutrino curves.

struction, the likelihood of the fit, the center of gravity of the hits and the vertical distance between the deepest and shallowest hit modules. The MLPfit package was used [18]. The network performance was optimized by varying the network architecture, the size of the training samples and minimization algorithms. An architecture of 8–40–1 with a hybrid linear minimization was found to give maximal efficiency.

The final event selection consisted of the following series of cuts: the number of hit channels, the number of 'early' hits ($t_{res} < -15$ ns), the number of hits used in the first-guess fit and the distance between the first and last direct hits projected on the track direction. For this last cut, the direct hit definition used was -15 ns $< t_{res} < 75$ ns. Fig. 1 shows an example of the relative efficiency for signal, background and data as a function of cut level, for one of the neutralino masses. Cut level 4 corresponds to the cut on the NN output, and the last level to the addition of the cuts just described, shown individually as the intermediate points between levels 4 and 5 in the plot. Fig. 2 shows the distribution of the cosine of the space angle, Ω, between the reconstructed tracks and
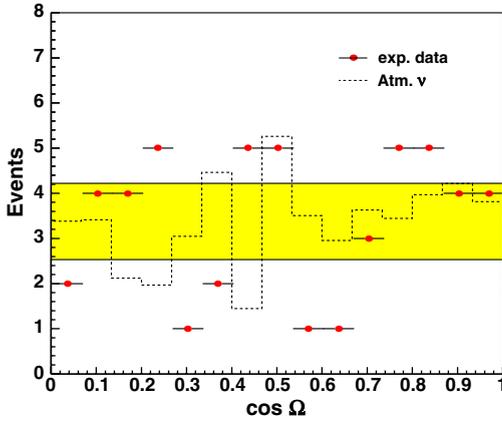
Fig. 2. Cosine of the space angle between the reconstructed track and the Sun position at final cut level for data and atmospheric neutrinos. The case shown is for the cut optimization for 500 GeV neutralinos (annihilation into W^+W^-). The shaded area shows the one standard deviation systematic uncertainty in the expected atmospheric neutrino distribution.

the direction of the Sun (after unblinding). The distribution is in agreement, both in shape and normalization, with the expectation from the atmospheric neutrino background, within the 25% overall systematics of the atmospheric neutrino flux [19] (indicated by the shaded band).

5. Systematic uncertainties

There are several systematic uncertainties in the detector effective volume that should be taken into account when calculating limits. The uncertainty in the optical module sensitivity contributes about 14%, while the detector calibration and the hardware simulation contribute about 5%. The largest contribution comes from the imprecise knowledge of the layered structure and the impurity contents of the ice, and is less than about 30% (with the exception of the softest spectrum, annihilation of 100 GeV neutralinos into $b\bar{b}$ where this uncertainty reaches about 50%). Uncertainties on the neutrino–nucleon cross-sections and in the simulation of muon energy loss contribute of the order of 5%. The overall systematic uncertainties in the detector effective volume lie between 20% and about 60% depending on the neutralino mass

model being tested (see [17] for details). The uncertainties have been incorporated in the limits using the method described in [20] with the unified Feldman–Cousins ordering scheme [21].

6. Results

Different angular bins around the position of the Sun for each neutralino mass and annihilation channel were used in the search for a signal. The bins were chosen as containing 90% of the signal, and they range from 5.5° for the harder neutrino spectra to 26° for the softest spectrum (100 GeV neutralinos annihilating into $b\bar{b}$). The off-source data in the declination band of the Sun were used to estimate the expected background at the Sun position. This procedure eliminates any effects of uncertainties in the background simulation and in the total normalization of the atmospheric neutrino flux. Table 1 summarizes the relevant numbers.

No evidence of a statistically significant excess of events from the direction of the Sun was found. Therefore, the number of observed events from that direction, together with the Poisson mean of the background expectation, were used to set limits on the neutrino flux at the Earth from neutralino annihilations in the Sun. We have followed the same prescription as in [8], starting from the directly measurable quantity, the neutrino-to-muon conversion rate, $\Gamma_{\nu\to\mu} = \mu_{90}/(V_{\mathrm{eff}}\epsilon t)$, where μ_{90} is the 90% CL signal upper limit, t is the livetime, ϵ the reconstruction efficiency and V_{eff} the effective volume of the detector at final cut level. The limit on the annihilation rate of neutralinos in the Sun, Γ_A, is proportional to $\Gamma_{\nu\to\mu}$, where the proportionality coefficient takes into account the production of muons through the neutrino–nucleon cross-section weighted by the different branching ratios of the $\tilde{\chi}_1^0\tilde{\chi}_1^0$ annihilation process and the corresponding neutrino energy spectra. From Γ_A we reach the limit on the muon flux at the Earth by taking into account that

$$\phi_\mu(E_\mu \geqslant E_{\mathrm{thr}}) = \frac{\Gamma_A}{4\pi D_\odot^2} \int_{E_{\mathrm{thr}}}^{\infty} \mathrm{d}E_\mu \frac{\mathrm{d}N_\mu}{\mathrm{d}E_\mu}, \tag{1}$$

Table 1
For each neutralino mass and annihilation channel the table shows: The number of data events, N_{data}, the number of expected atmospheric neutrinos in the declination band of the Sun, $N_{\text{atm}\nu}^{\text{MC}}$, the search bin, Ψ, the final number of data events and the estimated background in the search bin, N_{data}^{Ψ} and N_{bck}^{Ψ} respectively and the muon effective volume, V_{eff}. The last three columns show the 90% CL upper limit on the expected signal, μ_{90}, and the corresponding 90% CL limits on the annihilation rate at the center of the Sun and on the muon flux at the Earth, Γ_A and Φ_μ. The limits include systematic uncertainties. 'Soft' and 'hard' refer to annihilation into b$\bar{\text{b}}$ and W$^+$W$^-$ respectively

$m_{\tilde{\chi}_1^0}$ (GeV)	Channel	N_{data}	$N_{\text{atm}\nu}^{\text{MC}}$	Ψ (deg)	N_{data}^{Ψ}	N_{bck}^{Ψ}	V_{eff} (m^3)	μ_{90}	Γ_A (s^{-1})	Φ_μ (km^{-2} y^{-1})
100	Hard	39	42.7	11	1	2.5	4.2×10^4	2.3	8.6×10^{23}	2.5×10^4
	Soft	41	45.9	26	6	5.6	1.7×10^3	9.7	8.0×10^{26}	2.8×10^6
250	Hard	49	46.6	8	2	2.2	7.0×10^5	4.1	5.1×10^{22}	6.2×10^3
	Soft	53	49.4	10	4	2.7	5.3×10^4	8.9	5.5×10^{24}	7.2×10^3
500	Hard	51	48.5	7	1	2.0	1.7×10^6	2.5	1.1×10^{22}	2.4×10^3
	Soft	51	50.1	8	1	2.3	1.9×10^5	2.5	2.8×10^{22}	8.0×10^2
1000	Hard	50	49.3	6	1	1.7	2.8×10^6	2.9	8.5×10^{21}	2.2×10^3
	Soft	51	52.2	8	1	2.3	3.5×10^5	2.5	1.1×10^{23}	5.4×10^3
3000	Hard	48	49.3	5.5	1	1.5	2.8×10^6	3.1	1.4×10^{22}	2.3×10^3
	Soft	49	49.7	7	1	1.9	4.8×10^5	2.7	5.5×10^{22}	4.7×10^3
5000	Hard	51	47.8	5.5	1	1.6	2.6×10^6	2.9	1.9×10^{22}	2.3×10^3
	Soft	51	49.4	7	1	2.0	5.7×10^5	2.7	4.3×10^{22}	4.2×10^3

where $D_\odot$ is the distance to the Sun and dN_μ/dE_μ is the muon flux produced from the neutralino annihilations, including all MSSM model dependencies and interaction kinematics. E_{thr} is here an arbitrary threshold, that can be used to convert the measured flux limit (which is obtained for the actual detector energy threshold) to any other threshold. The last three columns of Table 1 show the Feldman–Cousins 90% upper limit on the expected signal and the corresponding 90% CL limits on the annihilation rate at the center of the Sun and on the muon flux at the Earth. All numbers include systematic uncertainties.

7. Discussion

Fig. 3 shows the AMANDA limits on the muon flux at the Earth from neutralino annihilations into W$^+$W$^-$ (hard channel) in the Sun as a function of neutralino mass, compared to the results of Baksan [22], MACRO [23] and Super-K [24] and theoretical predictions based on DARKSUSY. The limits have been rescaled to a common muon
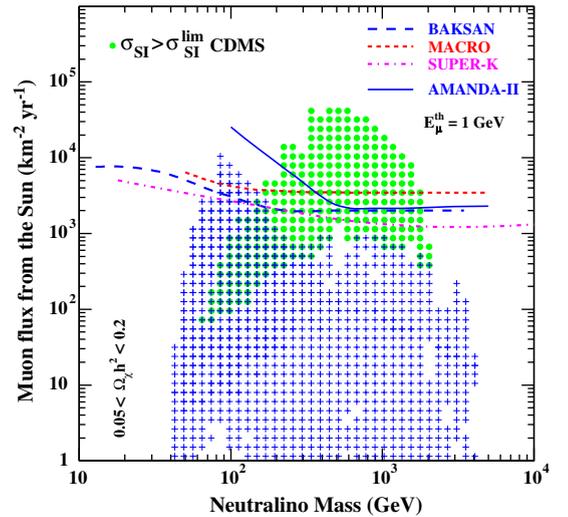

Fig. 3. Upper limits on the muon flux from the Sun, Φ_μ, from neutralino annihilations into W$^+$W$^-$ (hard channel) as a function of neutralino mass. The muon energy threshold has been extrapolated to a common value of 1 GeV. The dots show the models disfavored by recent direct search results from CDMS.

threshold of 1 GeV using the known energy spectrum of the neutralinos. The sparseness of the arrangement of the AMANDA strings (not less than 25 m between nearest neighbours) makes the detector less effective at lower neutrino energies, and leads to a worsening of the limit for neutralino masses below about 500 GeV. Above this mass, AMANDA, with the 144 days of live-time used for the present analysis, is already competitive with experiments with much longer exposure times (3.6 years of collected data for MACRO and 4.6 years for Super-K for example).

The symbols in the figure represent the predictions of DARKSUSY for given combinations of SUSY parameters. The models shown are only those which give a relic density within the current limits of allowed dark matter density in the universe, $0.05 < \Omega h^2 < 0.2$. The dots represent parameter combinations that are disfavored by the latest results from direct experiments setting limits on the neutralino–nucleon cross-section [25]. Although comparison between direct and indirect searches is not straightforward, the figure shows that current results from indirect searches are competitive in the high neutralino mass region.

Neutrino oscillations in the atmosphere (not included in the simulations) would tend to reduce the muon–neutrino flux and affect the total normalization of the background. Since we have used the measured neutrino flux off-source as an estimation of the background at the source position, the effect of oscillations is inherently included in the analysis. The atmospheric neutrino simulations were used as a confirmation that the analysis cuts selected atmospheric neutrinos and rejected the down-going atmospheric muons to the desired level before the unblinding of the dataset.

The DARKSUSY simulations did not include oscillations of the neutrinos on their way to the Earth. The effect of oscillations of neutrinos produced in the Sun on the final flux observed at the Earth has been discussed in [26] (and in [27] in a slightly different context). Detailed calculations in [26] found that the resulting muon flux at the Earth from low mass $(m_{\tilde{\chi}_1^0} < m_t)$ MSSM neutralino annihilations can be considerably affected by $\nu_\tau \leftrightarrow \nu_\mu$ oscillations in some scenarios. This is the case for MSSM models with important

annihilation branching ratios into $\tau^+\tau^-$, typically $B_{\tau\tau} > 0.1$. In such cases the muon flux at the Earth can be increased by a factor of about 2–4 with respect to the no-oscillation case. For higher neutralino masses, where the main annihilation channel can be through gauge bosons or heavy quarks, the effect of $\nu_\tau \leftrightarrow \nu_\mu$ oscillations is negligible, oscillations into ν_τ being compensated by ν_τ oscillating into ν_μ. Flavor mixing with ν_e both from ν_μ and ν_τ is suppressed by the small value of Δm_{21}^2 and the mixing angle $\sin^2 2\theta_{31}$ respectively, and does not play a role when considering the ν_μ flux from the Sun. Given the considerations above, the flux and annihilation rate limits presented in this article for the case of annihilations into W^+W^- would be practically unaffected if one were to consider oscillations. The results for the $b\bar{b}$ annihilation channel would also be unaffected for high neutralino masses $(m_{\tilde{\chi}_1^0} \gtrsim 200 \text{ GeV})$ and would worsen by a few percent for neutralino masses below 200 GeV.

Acknowledgements

References

[1] S.P. Martin. Available from: <hep-ph/9709356>.
[2] G. Bélanger et al., J. High Energy Phys. JHEP03 (2004) 012.
[3] K. Griest, M. Kamionkowski, Phys. Rev. Lett. 64 (1990) 615.

[4] W.H. Press, D.N. Spergel, Astrophys. J. 296 (1985) 679.
[5] J. Silk, K. Olive, M. Srednicki, Phys. Rev. Lett. 55 (1985) 257;
T. Gaisser, G. Steigman, S. Tilav, Phys. Rev. D 34 (1986) 2206.
[6] A. Gould, Astrophys. J. 328 (1988) 919.
[7] G. Jungman, M. Kamionkowski, K. Griest, Phys. Rep. 267 (1996) 195.
[8] J. Ahrens et al., Phys. Rev. D 66 (2002) 032006.
[9] J. Ahrens et al., Nucl. Instrum. Methods A 524 (2004) 169.
[10] P. Gondolo et al., J. Cosm. Astropart. Phys. 0407 (2004) 008.
[11] T. Sjöstrand, Comput. Phys. Commun. 82 (1994) 74.
[12] H.L. Lai et al., Phys. Rev. D 51 (1995) 1280;
H.L. Lai et al., Eur. Phys. J. C 14 (2) (2000) 187.
[13] P. Lipari, Astropart. Phys. 1 (1993) 195.
[14] D. Heck et al., FZKA report 6019, 1998. Available from: <http://ik1au1.fzk.de/~heck/corsika/>.
[15] Particle Data Group, Eur. Phys. J. 15 (2000) 1.
[16] D. Chirkin, W. Rhode, in: Proceedings of the 27th International Cosmic Ray Conference, Hamburg, Germany, 2001, HE2.02, p. 1017.

[17] Y. Minaeva, Ph.D. thesis, Stockholm University, 2004, ISBN 91-7265-882-7.
[18] J. Schwindling, B. Mansoulié. Available from: <http://schwind.home.cern.ch/schwind/MLPfit.html>.
[19] T. Gaisser, M. Honda, Ann. Rev. Nucl. Part. Sci. 52 (2002) 153.
[20] J. Conrad et al., Phys. Rev. D 67 (2003) 012002.
[21] A. Stuart et al.Kendall's Advanced Theory of Statistics, vol. 2, Oxford University Press, 1991;
G.J. Feldman, R.D. Cousins, Phys. Rev. D 57 (1998) 873.
[22] M.M. Boliev et al., in: H.V. Klapdor-Kleingrothaus, Y. Ramachers (Eds.), Proceedings of the International Workshop on Aspects of Dark Matter in Astrophysics and Particle Physics, Heidelberg, Germany, 1996, World Scientific, Singapore, 1997.
[23] M. Ambrosio et al., Phys. Rev. D 60 (1999) 082002.
[24] S. Desai et al., Phys. Rev. D 70 (2004) 083523, Erratum-ibid. D70 (2004) 109901.
[25] D.S. Akerib et al., Phys. Rev. Lett. 93 (2004) 211301.
[26] M. Kowalski, Phys. Lett. B 511 (2001) 119.
[27] P. Crotty, Phys. Rev. D 66 (2002) 063504.